

# Molecular Template-Directed Synthesis of Microporous Polymer Networks for Highly Selective CO<sub>2</sub> Capture

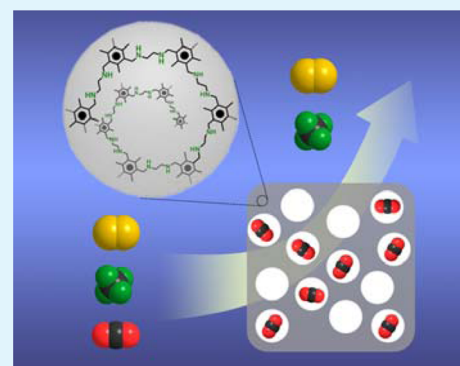
Yao-Qi Shi, Jing Zhu, Xiao-Qin Liu,\* Jian-Cheng Geng, and Lin-Bing Sun\*

State Key Laboratory of Materials-Oriented Chemical Engineering, College of Chemistry and Chemical Engineering, Nanjing Tech University, Nanjing 210009, China

## S Supporting Information

**ABSTRACT:** Porous polymer networks have great potential in various applications including carbon capture. However, complex monomers and/or expensive catalysts are commonly used for their synthesis, which makes the process complicated, costly, and hard to scale up. Herein, we develop a molecular template strategy to fabricate new porous polymer networks by a simple nucleophilic substitution reaction of two low-cost monomers (i.e., chloromethylbenzene and ethylene diamine). The polymerization reactions can take place under mild conditions in the absence of any catalysts. The resultant materials are interconnected with secondary amines and show well-defined micropores due to the structure-directing role of solvent molecules. These properties make our materials highly efficient for selective CO<sub>2</sub> capture, and unusually high CO<sub>2</sub>/N<sub>2</sub> and CO<sub>2</sub>/CH<sub>4</sub> selectivities are obtained. Furthermore, the adsorbents can be completely regenerated under mild conditions. Our materials may provide promising candidates for selective capture of CO<sub>2</sub> from mixtures such as flue gas and natural gas.

**KEYWORDS:** porous polymer networks, molecular template, CO<sub>2</sub> capture, selectivity, regeneration



## INTRODUCTION

Emission of carbon dioxide (CO<sub>2</sub>) contributes to global warming significantly, which has become an urgent environmental concern. Carbon capture and sequestration (CCS), a process to separate CO<sub>2</sub> from the combustion of fossil fuels, has been considered an effective way to control the concentration of atmospheric CO<sub>2</sub>.<sup>1–6</sup> Much attention has been paid to selective capture of CO<sub>2</sub> from mixtures such as flue gas (postcombustion) and natural gas (precombustion). For the combustion of fossil fuels and biomass, the content of CO<sub>2</sub> in flue gas is about 15%, whereas others are mainly composed of nitrogen (N<sub>2</sub>). In the case of landfill gas and natural gas, the main components are methane (CH<sub>4</sub>), CO<sub>2</sub>, N<sub>2</sub>, and a small amount of hydrocarbons. The existence of CO<sub>2</sub> reduces their reactivity and heating capacity, and it also causes corrosion of the relevant pipeline and equipment. As a result, the separation of CO<sub>2</sub> from gas mixtures containing N<sub>2</sub> and CH<sub>4</sub> is of growing interest from both academic and practical points of view.<sup>7–13</sup>

The conventional method to remove CO<sub>2</sub> is “wet scrubbing” by using aqueous amine (e.g., monoethanolamine, MEA) solutions.<sup>14</sup> However, this process has several inherent problems, such as high regeneration costs and erosion of the equipment. An alternative approach is adsorption by use of porous materials. The porous solids have specific heat capacities that are substantially less than those of aqueous solutions. Moreover, they are easier to handle and free of corrosion problems. These advantages make porous materials highly promising for CO<sub>2</sub> capture. In the last decades, metal–organic frameworks (MOFs)

have been reported to show outstanding capacities in CO<sub>2</sub> capture due to their large surface areas and high pore volumes. Unfortunately, most MOFs are unstable in high temperatures, moisture, and other harsh environments, which are difficult to meet the strict industrial requirements.<sup>3,15–25</sup> Fortunately, porous polymer networks (also known as covalent organic frameworks,<sup>26</sup> hyper cross-linked polymers,<sup>27</sup> conjugated microporous polymers,<sup>28</sup> polymer of intrinsic microporosity,<sup>29</sup> covalent triazine-based frameworks,<sup>30</sup> porous aromatic frameworks,<sup>31</sup> etc.), another type of adsorbents with comparable porosity, show much better physicochemical stability as a result of the covalent bonding of the framework construction. Therefore, many attempts have been made to the development of efficient porous polymer networks for CO<sub>2</sub> capture.<sup>32–37</sup>

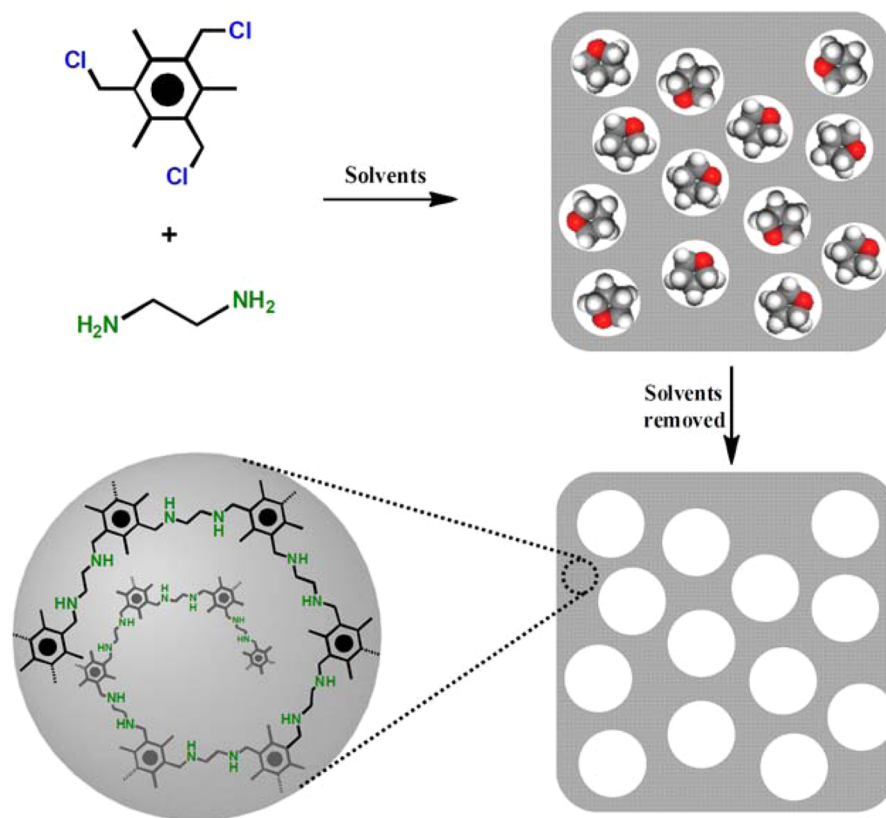
By a condensation reaction of 2,4,6-tris(4-aminophenyl)-1,3,5-triazine (TAPT) and the respective dianhydride building blocks in *m*-cresol, Senker's group<sup>30</sup> synthesized several triazine-based porous polyimide (TPI) polymer networks. The resulting TPI polymer networks exhibited good chemical and thermal stability as well as high CO<sub>2</sub> uptakes. Nevertheless, the monomer TAPT was prepared from the quite preliminary precursor 4-bromobenzonitrile via a series of tedious organic reactions. Through a Yamamoto-type Ullmann reaction containing quadrivalent Si and Ge, Ben et al.<sup>38</sup> reported the synthesis of

Received: August 29, 2014

Accepted: November 7, 2014

Published: November 17, 2014

Scheme 1. Monomers and Schematic Structure of Resultant Porous Polymer Networks



two porous aromatic frameworks (PAFs). These materials exhibit high surface areas and excellent adsorption ability to CH<sub>4</sub> and CO<sub>2</sub>. It should be stated that an expensive catalyst, bis(1,5-cyclooctadiene) nickel(0), namely Ni(COD)<sub>2</sub>, has to be employed in the polymerization process. Actually, complex monomers and/or expensive catalysts are commonly used for the synthesis of most reported porous polymer networks, which makes the synthetic process complicated, costly, and hard to scale up. Despite great efforts have been dedicated, fabrication of porous polymer networks from low-cost monomers via a catalyst-free and simple polymerization reaction remains a great challenge up to now.

Due to the polarizability and large quadrupole moment of CO<sub>2</sub>, CO<sub>2</sub>-philic groups, amines, are usually introduced to create strong interaction between the material and CO<sub>2</sub>. This approach has been proven to be effective in enhancing the enthalpy of CO<sub>2</sub> adsorption and the selectivity of CO<sub>2</sub>.<sup>39–43</sup> It should be stated that the type of amine has a significant effect on CO<sub>2</sub> adsorption with regard to selectivity and energy consumption for regeneration. Strong chemical interaction of primary amines has a negative impact on regeneration of adsorbents, while tertiary amines are unfavorable to adsorption capacity and selectivity of CO<sub>2</sub>. Therefore, secondary amines are ideal building blocks for porous polymer networks, and they can take the balance of high selectivity of CO<sub>2</sub> and energy-saving regeneration.<sup>44–50</sup>

In the present study, we developed a molecular template strategy to fabricate a series of new porous polymer networks by a simple nucleophilic substitution reaction of two monomers, that is, chloromethylbenzene and ethylene diamine (Scheme 1). In the synthetic systems, organic solvent molecules serve as the templates to direct the growth of porous polymer networks,

leading to the formation of well-defined micropores with the dimension of solvent molecules. The polymerization reactions can take place under mild conditions in the absence of any catalysts. Moreover, both monomers are low-cost and readily available. The resultant materials are interconnected with secondary amine groups, and present appropriate interaction for CO<sub>2</sub>, which is beneficial to both selective adsorption and energy-saving regeneration. Our results demonstrate that these materials are efficient for adsorption of CO<sub>2</sub>, whereas CH<sub>4</sub> and N<sub>2</sub> are barely adsorbed. As a result, an unusually high selectivity of CO<sub>2</sub> over N<sub>2</sub> and CH<sub>4</sub> is obtained. More importantly, these porous polymer networks can be completely regenerated under mild conditions, and the adsorption activity is well maintained even after six cycles.

## EXPERIMENTAL SECTION

**Materials Synthesis.** The monomer 2,4,6-tris(chloromethyl)-mesitylene (M1) was prepared according to a method reported previously.<sup>51</sup> The porous polymer networks were synthesized by a nucleophilic substitution reaction of M1 with ethylene diamine. In a typical process, M1 (0.561 g, 2 mmol) was dissolved in tetrahydrofuran (THF, 50 mL) and the solution was stirred vigorously, followed by the addition of ethylene diamine (0.180 g, 3 mmol). A glovebox is not necessary for the synthesis, while a large amount of water and CO<sub>2</sub> are not beneficial to the formation of polymer. As a result, the obtained solution was heated in a closed system (at 63 °C for 24 h). After the solution cooled to room temperature, the reaction mixture was centrifuged to remove the solvent, and the precipitate was treated with an ethanol/water (20 mL/20 mL) solution of KOH (1.008 g) at 45 °C for 12 h. The material was then washed with an ethanol/water solution for three times and dried at room temperature. The obtained white powder was denoted as P1. In a similar process, the porous polymer networks P2 and P3 were synthesized, by using 1,4-dioxane (DIO) and ethyl acetate (EA) as the solvents, respectively.

**Characterization.** Fourier transform infrared (IR) spectra were recorded on a Nicolet Nexus 470 spectrometer with a KBr wafer. The proportion of samples and KBr are 1:150. Solid state  $^{13}\text{C}$  cross-polarization (CP) magic angle spinning (MAS) nuclear magnetic resonance (NMR) spectra were measured on a Bruker AVANCE 400 spectrometer using densely packed powders of porous polymer networks in 4 mm  $\text{ZrO}_2$  rotors. Elemental analysis was carried out on an Elementar Vario EL elemental analyzer. Thermogravimetric (TG) analysis was performed using a thermobalance (STA-499C, NETZSCH). About 10 mg of sample was heated from room temperature to 800 °C in a flow of  $\text{N}_2$  (20 mL·min $^{-1}$ ). For the analysis of pore structure, two gas probes,  $\text{N}_2$  and  $\text{CO}_2$ , were employed. The adsorption measurements were undertaken using a Micromeritics ASAP 2020 surface area and pore size analyzer. The samples were degassed at 120 °C for 6 h before analysis, then the sample was backfilled with  $\text{N}_2$  and transferred to the analysis system.  $\text{N}_2$  adsorption was carried out at 77 K while  $\text{CO}_2$  adsorption analysis was carried out at 273 K. The specific surface areas for  $\text{N}_2$  and  $\text{CO}_2$  adsorption were calculated using the Brunauer–Emmett–Teller (BET) model over a relative pressure range of 0.01–0.10. Total pore volumes were calculated from the uptake at a relative pressure of 0.95. Pore size distributions were calculated from the adsorption isotherms by the Horvath–Kawazoe (HK) method.

**Adsorption Experiments.** Static adsorption experiments of  $\text{CO}_2$ ,  $\text{CH}_4$ , and  $\text{N}_2$  were conducted using an ASAP 2020 analyzer.  $\text{CO}_2$  (99.999%),  $\text{CH}_4$  (99.99%), and  $\text{N}_2$  (99.999%) gases were used for all adsorption measurements. Free space was measured using helium (99.999%), assuming that the helium is not adsorbed at any of the studied temperatures. Adsorption–desorption isotherms of  $\text{CO}_2$ ,  $\text{CH}_4$ , and  $\text{N}_2$  at 273 K were measured in an ice–water bath whereas isotherms at 298 K were measured in a water bath.

The isosteric heats of  $\text{CO}_2$  adsorption ( $Q_{\text{st}}$ ) were calculated from the  $\text{CO}_2$  adsorption isotherms at temperatures of 273 and 298 K, the data were simulated with a virial-type expression composed of parameters  $a_i$  and  $b_i$  that are independent of temperature according to eq 1. Generally, a nonlinear curve was obtained displaying the connection between  $\ln P$  and adsorption quantity ( $N$ ), from the fitting parameters results of  $a_i$ , the  $Q_{\text{st}}$  was calculated according to eq 2.<sup>52</sup>

$$\ln P = \ln N + \frac{1}{T} \sum_{i=0}^m a_i N^i + \sum_{i=0}^n b_i N^i \quad (1)$$

$$Q_{\text{st}} = -R \sum_{i=0}^m a_i N^i \quad (2)$$

To investigate the adsorption selectivity of  $\text{CO}_2$  over  $\text{CH}_4$  or  $\text{N}_2$  on porous polymer networks, the selectivity is defined as  $S = (x_1/y_1)/(x_2/y_2)$ , where  $x_1$  and  $y_1$  ( $x_2$  and  $y_2$ ) are the molar fractions of component 1 (component 2) in the adsorbed and bulk phases, respectively.<sup>53</sup> The ideal adsorption solution theory (IAST) of Myers<sup>54</sup> has been reported to predict binary gas mixture adsorption in porous materials accurately, and so far, many theoretical models combined with the IAST have been proposed to describe the adsorption data, such as Langmuir model, dual-site Langmuir mode (DL), dual-site Langmuir–Freundlich mode (DLF), and so on. Herein, the DL model was chosen to fit the adsorption isotherms, and then DL-IAST was utilized to estimate  $\text{CO}_2/\text{N}_2$  and  $\text{CO}_2/\text{CH}_4$  selectivities of porous polymer networks. In the calculation, a  $\text{CO}_2/\text{N}_2$  ratio of 15/85 and a  $\text{CO}_2/\text{CH}_4$  ratio of 50/50 were used, which are a typical composition of flue gas emitted from coal-fired power plants and a general feed composition of landfill gas, respectively. The regeneration experiments were carried out on an ASAP 2020 analyzer, the sample was saturated with  $\text{CO}_2$  up to 1 bar at 273 K followed by evacuating at 60 °C, and the adsorption capacity of regenerated adsorbents were then measured again.

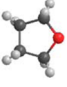
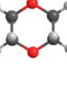
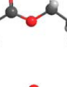
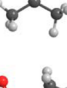
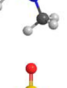
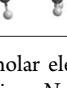
The dynamic breakthrough curve measurements of porous polymer networks were carried out in a steel tube column with an internal diameter of 5 mm. The powder sample was packed with a length of 50 mm. The column was placed into an oven and was heated at 393 K with an argon flow of 2 mL·min $^{-1}$  for 4 h before the measurements. After the column cooled down to room temperature, the gas flow was switched to the desired gas mixture at the same flow rate at 0.2 MPa. The column

downstream was monitored using a Hiden mass spectrometer. The complete breakthrough of  $\text{CO}_2$  and other species was indicated by the downstream gas composition reaching that of the feed gas. In the experiments, binary mixture gases were prepared with a  $\text{CO}_2/\text{N}_2$  ratio of 15/85 and a  $\text{CO}_2/\text{CH}_4$  of 50/50, which are typical composition of flue gas emitted from coal-fired power plants and general feed composition of landfill gas, respectively.

## RESULTS

**Synthesis and Structural Characterization.** Porous polymer networks were synthesized through the nucleophilic substitution reaction of chloromethylbenzene with ethylene diamine (Scheme 1). Six solvents with different molecular size and polarity, namely THF, DIO, EA, ACE, DMF, and DMSO, were attempted as shown in Table 1. The monomers can dissolve

**Table 1.** Physicochemical Properties of Solvents and Resultant Products

Solvent	Structure	Molecular diameter (Å)	$E_{\text{T}}(30)^a$ (kcal·mol $^{-1}$ )	Product
Tetrahydrofuran (THF)		4.12	37.4	P1
1,4-Dioxane (DIO)		4.80	36.0	P2
Ethyl acetate (EA)		5.58	38.1	P3
Acetone (ACE)		4.30	42.2	–
<i>N,N</i> -Dimethyl formamide (DMF)		4.60	43.8	–
Dimethyl sulfoxide (DMSO)		4.16	45.1	–

<sup>a</sup> $E_{\text{T}}(30)$  value is the molar electronic transition energies of dissolved solvatochromic pyridinium *N*-phenolate betaine dye, which is used as the parameter of solvent polarity.<sup>55</sup>

in all of the above solvents, leading to the formation of clear colorless solutions at the beginning of reactions. By using THF, DIO, and EA as solvents, white powders can be obtained as the target products. In the presence of ACE, DMF, and DMSO, nevertheless, no solid products appeared under the same reaction conditions, indicating that no polymerization reactions occurred at all. Apparently, solvents play an important role in the synthesis of porous polymer networks. Taking into account that the hydrolysis of EA is possible under polymerization conditions due to the formation of HCl, the liquid phase after polymerization was analyzed by gas chromatography (GC). As shown in Figure S1 (Supporting Information), no obvious difference can be observed between the liquid after reaction and pure EA. This suggests that EA is stable under the reaction conditions, which may be related to the interaction of HCl with amines in polymers. Triethylamine ( $\text{Et}_3\text{N}$ ) was used to capture HCl that generated in the polymerization process. The adsorption capacity of obtained material is apparently lower than the original material post-



treated with KOH (Figure S2, Supporting Information), which indicates that  $\text{Et}_3\text{N}$  is not efficient for the capture of HCl generated during synthesis. Various methods such as IR spectra, solid state  $^{13}\text{C}$  CP MAS NMR spectra, and elemental analysis were then employed to characterize these porous polymer networks.

As shown in Figure 1, the IR spectrum of M1 displays strong bands at  $600\text{--}800\text{ cm}^{-1}$  due to the C–Cl stretching vibrations. In

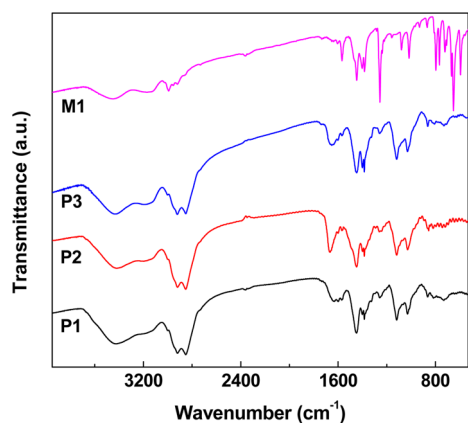


**Figure 1.** IR spectra of the monomer M1 and porous polymer networks P1, P2, and P3.

the IR spectra of P1, P2, and P3, however, these bands diminish to an undetected level, suggesting the cleavage of C–Cl bonds in the process of polymerization. Two weak bands at  $2916$  and  $2846\text{ cm}^{-1}$ , representing the stretching vibrations of  $-\text{CH}_2-$ , can be observed in the spectrum of M1. Their intensity is greatly enhanced after polymerization, which is due to the connection of  $-\text{CH}_2-$  groups from the monomer diamine. The products P1, P2, and P3 give two new bands at  $1104$  and  $3428\text{ cm}^{-1}$ , which can be ascribed to the C–N and N–H stretching vibrations, respectively. IR spectra of the monomer and products clearly show the cleavage of C–Cl bonds, the formation of C–N bonds, and the enhancement of  $-\text{CH}_2-$  groups. This demonstrates that the porous polymer networks were fabricated through a nucleophilic substitution reaction, as shown in Scheme 1. The band at  $1640\text{ cm}^{-1}$  originated from primary amine groups ( $-\text{NH}_2$ ) are detected on the products. This reveals that only one  $-\text{NH}_2$  in some diamines reacts with M1 and forms  $-\text{NH}-$ , while the other  $-\text{NH}_2$  becomes a pendant group in the products. It is easy to understand that the lower band intensity of  $-\text{NH}_2$  mirrors a higher polymerization degree of porous polymer networks. On the other hand, the intensity of the band at  $3428\text{ cm}^{-1}$  (N–H) is the higher of the polymerization degree should be. By combining the bands of  $-\text{NH}_2$  with N–H, it is reasonable that P1 with an intenser N–H band and a weaker  $-\text{NH}_2$  band has the highest polymerization degree among the three porous polymer networks.

Figure 2 displays the solid state  $^{13}\text{C}$  CP MAS NMR spectra of porous polymer networks. The three porous polymer networks present similar spectra, despite that different solvents were used in the synthetic process. All of the spectra give a peak at  $133.7\text{ ppm}$ , which is assigned to the  $\text{sp}^2\text{ C}$  in benzene rings. For the carbon atoms of methyl directly connected to benzene rings, they present a peak at  $14.8\text{ ppm}$ . The NMR peaks of carbon atoms connected to alkyl carbon and nitrogen are combined, which produces a broad peak at  $50.2\text{ ppm}$ . The elemental analysis was also conducted and the results are shown in Table 2. The

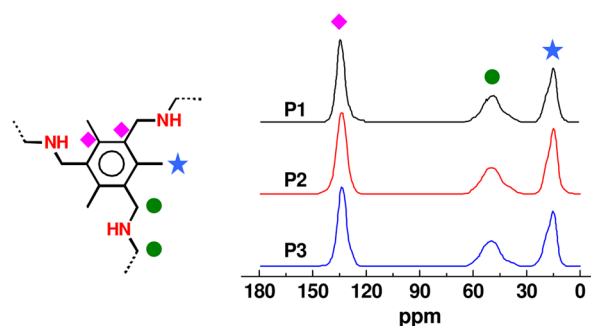


**Figure 2.** Solid state  $^{13}\text{C}$  CP MAS NMR spectra of porous polymer networks P1, P2, and P3.

products mainly consist of three elements, that is, carbon, nitrogen, and hydrogen. The nitrogen contents of around 12 wt % were observed in the porous polymer networks, indicating the successful introduction of nitrogen that may act as active species for the adsorption of  $\text{CO}_2$ . The IR spectra, together with NMR and elemental analysis results, demonstrate the successful fabrication of porous polymer networks through nucleophilic substitution reactions.

The pore structure of porous polymer networks was first evaluated by  $\text{N}_2$  adsorption at  $77\text{ K}$ . The isotherms show that the  $\text{N}_2$  uptakes at relative pressures lower than 0.8 are quite low, and the uptakes increase greatly at relative pressures higher than 0.8 (Figure S3, Supporting Information). Supercritical  $\text{CO}_2$  activation is a good method to maintain some pores that may be destroyed during thermal activation.<sup>56</sup> The polymers were thus activated using supercritical  $\text{CO}_2$ . The  $\text{N}_2$  uptake can be enhanced slightly, while the effect of supercritical  $\text{CO}_2$  is not as obvious as that reported in literature.<sup>56</sup> These results suggest that  $\text{N}_2$  is difficult to enter the pores of porous polymer networks, while with the increase of pressure, adsorption occurs on the outer surface and/or pores between aggregated particles. Correspondingly, the BET surface areas calculated from  $\text{N}_2$  adsorption are quite low. For instance, the material P1 only has a surface area of  $10.7\text{ m}^2\cdot\text{g}^{-1}$  (Table 2). Because the molecular size of  $\text{CO}_2$  ( $3.30\text{ \AA}$ ) is smaller than that of  $\text{N}_2$  ( $3.64\text{ \AA}$ ),  $\text{CO}_2$  was employed to probe the pore structure. The adsorption of  $\text{CO}_2$  at  $273\text{ K}$  offers a valid complementary method to study the porosity of material, in particular, the narrow micropores.<sup>37,57</sup> Unlike  $\text{N}_2$  adsorption, a large number of  $\text{CO}_2$  can be adsorbed at low relative pressures as shown in Figure 3. All of the materials show a type I isotherm according to IUPAC classification with characteristically steep uptake at low relative pressure. This suggests the microporous property of materials. The  $\text{CO}_2$  uptake on P1 is obviously higher than that on P2 and P3. In comparison with  $\text{N}_2$  adsorption, more valid textural parameters can be obtained by  $\text{CO}_2$  adsorption. Take P1 as an example, the surface area from  $\text{CO}_2$  adsorption is  $99.9\text{ m}^2\cdot\text{g}^{-1}$  (Table 2). This indicates that the pore diameter of P1 is larger than  $\text{CO}_2$  while smaller than  $\text{N}_2$ . As a result, the polymer can have high  $\text{CO}_2$  adsorption ability and low  $\text{N}_2$  adsorption ability, leading to a high selectivity of  $\text{CO}_2/\text{N}_2$ . Despite of the probe molecules, similar orders of pore diameters and pore volumes are observed. Apparently, the material P1 exhibits a smaller pore diameter and a larger pore volume in contrast with P2 and P3.

The thermal stability of porous polymer networks is examined by TG. As given in Figure 4, the weight losses at about  $100\text{ }^\circ\text{C}$  ascribed to the desorption of adsorbed water are negligible for all the materials, which indicates the hydrophobicity of porous

Table 2. Textural Properties and Elemental Analysis of Porous Polymer Networks

sample	$S_{\text{BET}}^a$ ( $\text{m}^2\cdot\text{g}^{-1}$ )	$V_p^a$ ( $\text{cm}^3\cdot\text{g}^{-1}$ )	$D_p^a$ ( $\text{\AA}$ )	elemental analysis (wt %)		
				N	C	H
P1	99.9 (10.7)	0.073 (0.026)	3.6 (5.6)	12.14	71.77	9.22
P2	56.7 (8.1)	0.051 (0.017)	4.3 (5.9)	11.90	70.31	8.99
P3	50.1 (9.4)	0.050 (0.019)	4.1 (5.7)	11.98	72.83	9.33

<sup>a</sup>The parameters were measured by  $\text{CO}_2$  adsorption at 273 K, whereas the parameters in parentheses were measured by  $\text{N}_2$  adsorption at 77 K.

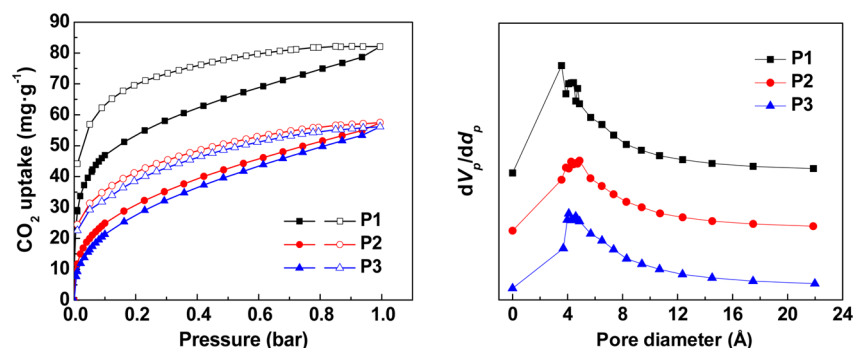


Figure 3.  $\text{CO}_2$  adsorption–desorption isotherms at 273 K. Pore size distributions were calculated from adsorption branches by the HK method.

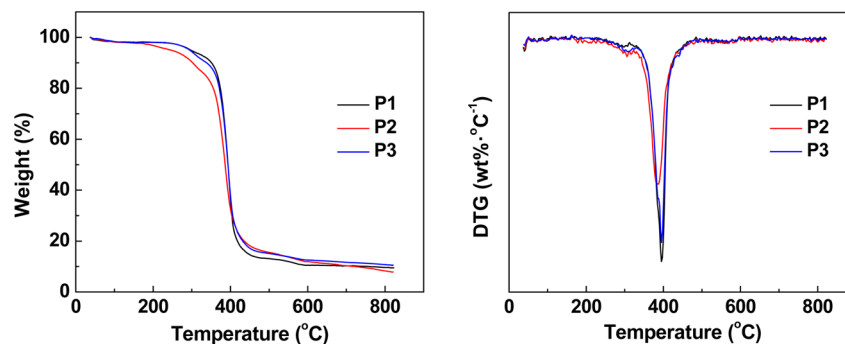


Figure 4. TG and DTG curves of porous polymer networks P1, P2, and P3.

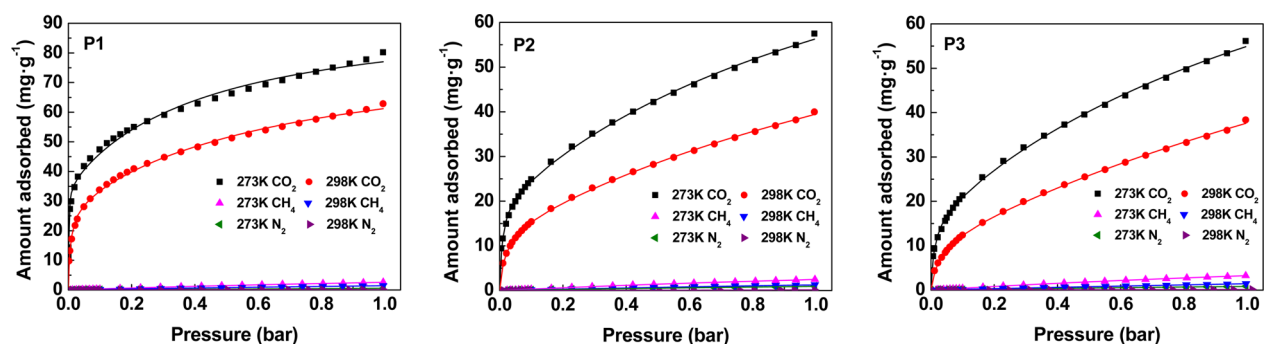


Figure 5. Adsorption isotherms of  $\text{CO}_2$ ,  $\text{CH}_4$ , and  $\text{N}_2$  on porous polymer networks P1, P2, and P3 at different temperatures. The lines are fitted results by use of the DL model.

polymer networks. The hydrophobicity/hydrophilicity of materials was also studied by the static water contact angle. The contact angle of a typical polymer P1 is  $63^\circ$ , as shown in Figure S4 (Supporting Information). For inorganic porous materials, due to surface hydrophilicity, the water droplet can easily penetrate into the bulk in the contact angle measurement, and disappeared within several seconds. In the case of organic polymers, however, the contact angles are usually higher than  $90^\circ$ . The presence of hydrophilic groups (such as acrylic acid, amines, and alumina) can lead to the decrease of contact angle as

reported in the literature.<sup>58,59</sup> Hence, it is easy to understand that the present materials show a contact angle higher than inorganic materials but lower than pure organic polymers. The predominant decomposition of frameworks takes place at about  $400^\circ\text{C}$ , followed by a gradual weight loss up to  $600^\circ\text{C}$ . The final weight stays steady at about 10% of the original weight of materials, which may be due to the formation of carbon. A slight weight loss at  $200\text{--}400^\circ\text{C}$  can be observed for P2, which is absent in other materials. In addition, the decomposition of P1 and P3 shows a sharp DTG peak at  $396^\circ\text{C}$ , whereas that of P2 is

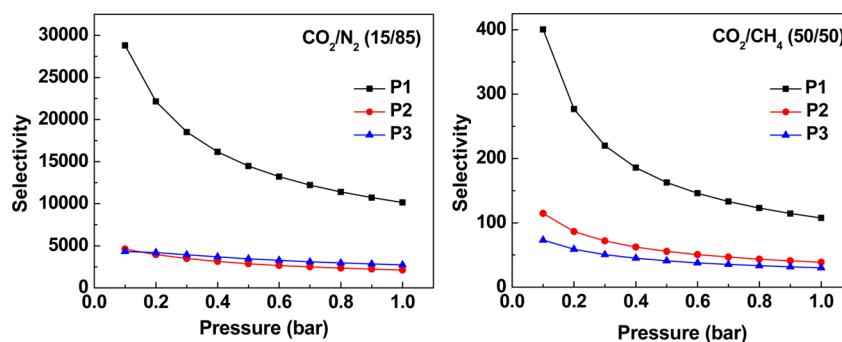


Figure 6. IAST selectivity of  $\text{CO}_2/\text{N}_2$  and  $\text{CO}_2/\text{CH}_4$  on porous polymer networks at 298 K.

at 385 °C. These results reflect that P1 and P3 are more stable as compared with P2.

**Static Adsorption Behavior of  $\text{CO}_2$ ,  $\text{CH}_4$ , and  $\text{N}_2$ .** The adsorption behavior of  $\text{CO}_2$ ,  $\text{CH}_4$ , and  $\text{N}_2$  on different materials was systematically studied. P1 has the highest adsorption capacity on  $\text{CO}_2$  among the three porous polymer networks in two different temperatures (Figure 5). For example, the uptakes of  $\text{CO}_2$  on P2 and P3 are 57.6 and 56.2  $\text{mg}\cdot\text{g}^{-1}$ , respectively, at 273 K. Under the same conditions, the uptake of  $\text{CO}_2$  on P1 reaches 82.1  $\text{mg}\cdot\text{g}^{-1}$ , which is obviously higher than that on P2 and P3. The adsorption capacity of P1 is comparable to some reported adsorbents such as porphyrin porous polymer CuPor-BPDC (55.0  $\text{mg}\cdot\text{g}^{-1}$ ),<sup>50</sup> microporous MOF  $\{[\text{Ni}(\text{L})_2]\cdot 4\text{H}_2\text{O}\}_n$  (56.2  $\text{mg}\cdot\text{g}^{-1}$ ),<sup>16</sup> conjugated microporous polymer CMP-1- $\text{NH}_2$  (70.4  $\text{mg}\cdot\text{g}^{-1}$ ),<sup>60</sup> porous electron-rich covalent organonitridic framework PECONF-1 (81.8  $\text{mg}\cdot\text{g}^{-1}$ ),<sup>61</sup> and porous polymer network PPN-6 (88.4  $\text{mg}\cdot\text{g}^{-1}$ ).<sup>62</sup> MEA is the most well-studied alkanolamine for  $\text{CO}_2$  capture applications and is usually dissolved in water at a concentration of about 20–30 wt %. The reaction of 2 equiv of MEA with  $\text{CO}_2$  results in the formation of an anionic carbamate species and a corresponding ammonium cation. Hence, the  $\text{CO}_2$  uptake of an MEA solution is between 1.6 and 2.4  $\text{mmol}\cdot\text{g}^{-1}$ , depending on the specific concentration. The  $\text{CO}_2$  uptake of P1 was calculated to be 1.8  $\text{mmol}\cdot\text{g}^{-1}$ , which is comparable to the MEA solution. In contrast to  $\text{CO}_2$ , the other gases  $\text{CH}_4$  and  $\text{N}_2$  are barely adsorbed on the porous polymer networks. At 273 K, the uptake of  $\text{CH}_4$  on P1 is only 2.6  $\text{mg}\cdot\text{g}^{-1}$ , while that of  $\text{N}_2$  is negligible (0.6  $\text{mg}\cdot\text{g}^{-1}$ ). The same trend is also found on P2 and P3. The uptake of  $\text{CH}_4$  and  $\text{N}_2$  on the present materials are lower than common porous materials reported in literature. These results indicate a high selectivity of  $\text{CO}_2$  over  $\text{CH}_4$  and  $\text{N}_2$ . As can be seen from  $\text{CO}_2$  adsorption isotherms, an initial steep increase in  $\text{CO}_2$  uptake at low pressure is observed, which suggests the presence of high-affinity binding sites (chemisorbed sites) for  $\text{CO}_2$ . With the increase of pressure, the  $\text{CO}_2$  uptake keeps increasing, indicating that physically adsorbed sites also exist in the polymers. IR spectra of P1 before and after  $\text{CO}_2$  adsorption were further recorded, shown in Figure S5 (Supporting Information). The band at 3428  $\text{cm}^{-1}$  that is ascribed to the N–H stretching vibration is weakened obviously due to the adsorption of  $\text{CO}_2$ . The IR results thus confirmed the presence of chemisorbed sites in the polymers.

To estimate the selectivity of  $\text{CO}_2/\text{N}_2$  and  $\text{CO}_2/\text{CH}_4$ , the DL-IAST model is employed. The fitting parameters of the DL model are shown in Tables S1–S3 (Supporting Information). The results of IAST selectivity are displayed in Figures 6 and S6 (Supporting Information). All porous polymer networks exhibit high adsorption selectivities of  $\text{CO}_2$  over  $\text{N}_2$  and  $\text{CH}_4$ . At 298 K

and 1 bar, the IAST selectivity of  $\text{CO}_2/\text{N}_2$  on P1 can reach 10139, which is higher than that on P2 (2113) and P3 (2736). Also, the selectivity of  $\text{CO}_2/\text{CH}_4$  on P1 is higher than that on P2 and P3. To the best of our knowledge, the material P1 shows the highest  $\text{CO}_2/\text{N}_2$  selectivity among the reported materials up to now. This selectivity is apparently higher than some well-known materials such as metal–organic frameworks SIFSIX-3-Zn (1818)<sup>15</sup> and Mg-MOF-74 (352),<sup>63</sup> porous polymer networks PPN-6- $\text{CO}_2$ DETA (442),<sup>8</sup> and zeolite 13X (220).<sup>64</sup>

To further understand the affinity of polymers and  $\text{CO}_2$ , the isosteric heat of adsorption is calculated from the isotherms at 273 and 298 K, shown in Figure 7. The nonlinear curve fitting

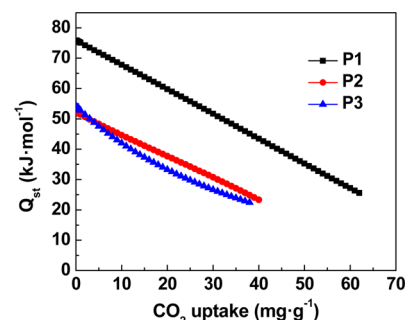
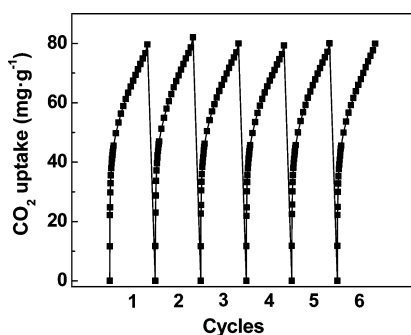


Figure 7.  $\text{CO}_2$  isosteric heat of adsorption of porous polymer networks P1, P2, and P3.

results of isotherms by the virial-type equation are shown in Figures S7–S9 (Supporting Information). At zero loading, the heat of adsorption of P1 reaches 75.9  $\text{kJ}\cdot\text{mol}^{-1}$ , whereas that of P2 (52.3  $\text{kJ}\cdot\text{mol}^{-1}$ ) and P3 (54.2  $\text{kJ}\cdot\text{mol}^{-1}$ ) is somewhat lower. As  $\text{CO}_2$  uptake increases, the heat of adsorption declines significantly, which may be caused by the continuous occupation of active sites with the increase of uptake.

Taking into account that the recyclability is crucial to the practical application of adsorbent, regeneration of porous polymer networks was carried out. As shown in Figures 8 and S10 (Supporting Information), no loss of activity is observed even after six cycles, demonstrating the excellent recyclability of present materials. It is worth noting that the saturated adsorbents were regenerated at only 60 °C for 100 min. These mild conditions are sufficient to recover the adsorption capacity completely. This can be attributed to the use of secondary amines as building blocks of adsorbents, which offers an appropriate  $\text{CO}_2$ -adsorbent interaction. Lu et al.<sup>8</sup> reported a porous polymer network tethered with primary amines, namely PPN-6- $\text{CH}_2$ DETA. The lower limit for the regeneration of adsorbents is 80 °C for 100 min, which is severer as compared with present



**Figure 8.** Six cycles regeneration experiment of CO<sub>2</sub> adsorption over the adsorbent P1.

materials constructed with secondary amines. By using chemical activation of polyindole nanofibers, Saleh et al.<sup>65</sup> prepared nitrogen-doped microporous carbon materials for CO<sub>2</sub> capture. Although a temperature of 150 °C is required for the regeneration of adsorbents, a slight loss of adsorption capacity can be observed after 10 cycles. The excellent recyclability, along with mild regeneration conditions, makes the present adsorbents highly promising for practical applications, aiming to develop new, energy-efficient carbon capture processes.

**Dynamic Breakthrough Curve Measurements.** For bulk separation of gas mixtures in the process of pressure swing adsorption (PSA) and temperature swing adsorption (TSA), dynamic breakthrough curves are quite useful to assess the performance of a new adsorbent. Two binary gas mixtures, namely CO<sub>2</sub>/N<sub>2</sub> (15/85) and CO<sub>2</sub>/CH<sub>4</sub> (50/50), were used for column breakthrough curve measurements. The results are illustrated in Figures 9, S11, and S12 (Supporting Information). In the case of a CO<sub>2</sub>/N<sub>2</sub> mixture, N<sub>2</sub> is the first gas to break through the column at about 20 s, which is understandable because N<sub>2</sub> is only weakly adsorbed on P1. It is worthy of note that the breakthrough of CO<sub>2</sub> is 450 s, which is much later than N<sub>2</sub>. A roll-up of N<sub>2</sub> can be seen from the breakthrough curve, which is displaced by CO<sub>2</sub> when CO<sub>2</sub> becomes the most adsorbed gas. Likewise, CH<sub>4</sub> is the weak adsorption ingredient in the case of a CO<sub>2</sub>/CH<sub>4</sub> mixture, and can break through the column first at about 80 s. This breakthrough time is obviously earlier than that of CO<sub>2</sub> (300 s). A roll-up of CH<sub>4</sub> is observed in the breakthrough curve, and is larger than that of N<sub>2</sub>. This is caused by the higher content of CH<sub>4</sub> in the binary gas mixture. In comparison with P2 and P3, the selectivity of CO<sub>2</sub>/N<sub>2</sub> and CO<sub>2</sub>/CH<sub>4</sub> on P1 is higher. For example, the breakthrough time of CO<sub>2</sub> on P1 is 450 s, which is longer than P2 (330 s) and P3 (360 s). The dynamic breakthrough curves are in good agreement with

the static adsorption results, and give further evidence of the high potential of present porous polymer networks in industrial applications.

## DISCUSSION

By use of a nucleophilic substitution reaction of chloromethylbenzene and diamine, a series of porous polymer networks are successfully fabricated. The reaction of chloromethylbenzene with amine group results in the formation of new C–N bonds along with hydrogen chloride as a byproduct. As a result, a large number of secondary amine groups are generated; they perform as bridges to connect benzene rings (Scheme 1). A continuous spatial polymer network is thus constructed. The network is made up of not only rigid groups (benzene rings) but also flexible linkages (C–C and C–N single bonds). In the synthetic process, it should be hard to form pores owing to the random orientation of flexible linkages. Interestingly, the present porous polymer networks exhibit relatively uniform pores with a size close to solvent molecules, which indicates that solvents play an important role in the formation of porous polymer networks. In addition to the function of reaction medium, the solvents are deemed to act as molecular templates, directing the growth of materials. The utilization of molecular templates to direct the formation of polymers has already been reported. The key point is the interaction between template and monomer, which can be demonstrated by UV absorption.<sup>66,67</sup> The UV absorption spectra of monomers in solvents were thus recorded. As shown in Figure S13 (Supporting Information), the redshift of ethylene diamine in THF was clearly observed, implying an association between the monomers and solvent molecules via hydrogen bonding. This gives further evidence of the templating role of solvent molecules. The interaction between solvent molecules and precursors lead to the positioning of the building blocks of polymers. The solvent molecules thus played a directing role, making polymer growth proceed in continuous solvent phase. A polymer intermediate with the pores occupied by solvents is thus fabricated. After the removal of solvents, porous polymer networks with pore dimensions of solvent molecules are produced.

It is interesting to note that the properties of polymers (e.g., polymerization degree, pore structure, and thermal stability) are different, despite that the same monomers and reaction conditions are employed for the synthesis. As a result, the properties of polymers should be strongly dependent on solvents used. To dissolve the two monomers in the present study, polar solvents are evidently required. A collection of polar solvents are thus attempted, as listed in Table 1. To compare the polarity of solvents quantitatively,  $E_T(30)$ , the molar electronic transition

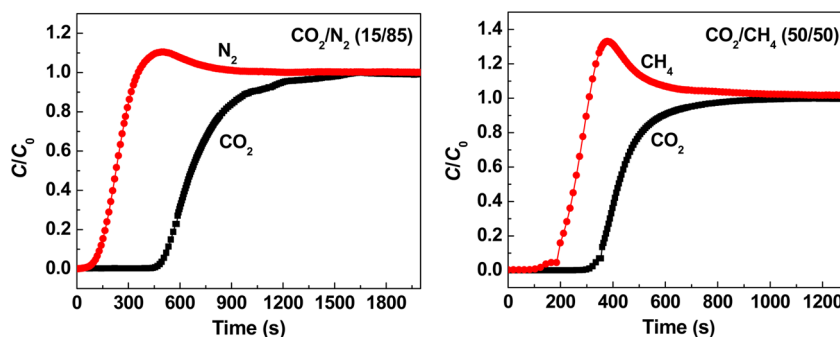


**Figure 9.** Dynamic breakthrough curves of CO<sub>2</sub>/N<sub>2</sub> and CO<sub>2</sub>/CH<sub>4</sub> over the adsorbent P1.



energy of dissolved solvatochromic pyridinium *N*-phenolate betaine dye, is applied.<sup>55</sup> A high  $E_T(30)$  value corresponds to high solvent polarity. As shown in Table 1, the  $E_T(30)$  values of different solvents vary from 36.0 to 45.1 kcal·mol<sup>-1</sup>. It is worth noting that solvents (THF, DIO, and EA) with an  $E_T(30)$  value lower than 38.1 kcal·mol<sup>-1</sup> favor the formation of polymers. On the contrary, for the solvents (ACE, DMF, and DMSO) with an  $E_T(30)$  value higher than 42.2 kcal·mol<sup>-1</sup>, no products can be formed at all. That means, as the reaction medium, solvents with too high polarity are harmful. A solvent with high polarity has strong interaction with the monomers. When the  $E_T(30)$  value is higher than 42.2 kcal·mol<sup>-1</sup>, such interaction may become comparable to the interaction between two monomers and thus hinder the polymerization reactions. Besides, even if some fragments were yielded from several monomer molecules, the high polarity of solvent may lead to the dissolution of these fragments. Apparently, the polarity of solvents is essential to the fabrication of porous polymer networks.

In addition to polarity, the molecular sizes of solvents are considered to be another factor affecting the fabrication of porous polymer networks. When THF is used as the solvent, the polymer P1 can be obtained. The pore size of P1 is 3.6 Å calculated from CO<sub>2</sub> adsorption, whereas that of P1 is 5.6 Å calculated from N<sub>2</sub> adsorption. The HK model is utilized to calculate the pore size for both CO<sub>2</sub> and N<sub>2</sub> adsorption. For the calculation of pore size distribution, various probe molecules and different methods could be used. The use of different probe molecules and methods may lead to different results. It should be normal because the pore structure for amorphous materials is complicated. Taking account of the accuracy of measurements and models, it is reasonable that the pore size of P1 is consistent with the molecular size of THF (4.12 Å). When solvents (i.e., DIO and EA) with larger molecular sizes are employed, the pore sizes of resultant polymers increase. By comparing Tables 1 and 2, it could be found that the pore size distribution of polymers is not completely consistent with the molecular size of solvents. Hence, the molecular size of solvent is not the unique factor influencing the pore size of polymer. In addition to molecular size, the polarity of solvents also has an effect on the formation of polymers. The rate of polymerization is very important to optimize porosity if the used solvents could affect this rate. It is found that the rate of polymerization in EA is a little higher than that in THF and DIO, but in general, there is no obvious difference for different solvents. As a result, the rate of polymerization caused by the used solvents should have a minor effect on porosity of polymer in the present study. As a result, it is postulated that the small molecular size of THF, together with the proper polarity, endows the resultant polymer P1 with the small pore size and high polymerization degree. The high polymerization degree of P1 is responsible for the large pore volume, high nitrogen content, and high thermal stability. On the basis of the above-mentioned analysis, it is conclusive that the properties of porous polymer networks strongly depend on the molecular size and polarity of solvents.

As described above, the present porous polymer networks exhibit excellent selective adsorption capacity on CO<sub>2</sub>. Under the same conditions, the uptakes of CH<sub>4</sub> and N<sub>2</sub> are neglectable. The high selectivity can be attributed to two factors, that is, the presence of abundant amine groups in frameworks and the appropriate pore sizes of polymers. First, secondary amines are typical CO<sub>2</sub>-philic sites, and can build strong interaction between CO<sub>2</sub> and polymers. This kind of interaction is absent in the case of CH<sub>4</sub> and N<sub>2</sub> as adsorbate molecules. Second, the dynamic

diameter of CO<sub>2</sub> is 3.30 Å, and is smaller than that of CH<sub>4</sub> (3.80 Å) and N<sub>2</sub> (3.64 Å). More importantly, the pore sizes of present adsorbents are quite close to the diameters of these adsorbate molecules. Accordingly, the effect of molecule sieving emerges on the present adsorption system. CO<sub>2</sub> with a small molecular size is easy to enter the pores of adsorbents, whereas the access of CH<sub>4</sub> and N<sub>2</sub> to the pores are relatively difficult. Based on the analysis above, it is easy to understand that P1 shows the highest selectivity of CO<sub>2</sub> over CH<sub>4</sub> and N<sub>2</sub> among the porous polymer networks. The largest content of amine groups in P1 is considered the first factor. In addition, the pore size of P1 is smaller than that of P2 and P3, and the effect of molecule sieving should be more obvious. In short, the excellent selective adsorption capacity of present materials on CO<sub>2</sub> is related to amine groups in their frameworks as well as proper sizes of the pores.

Despite the many efforts that have been made, so far, low-cost synthesis of porous polymer networks is still an open question from the viewpoints of monomers and catalysts. In this study, we design a molecular template strategy to construct porous polymer networks through a nucleophilic substitution reaction. Both monomers (chloromethylbenzene and ethylene diamine) are inexpensive and readily available. More importantly, the polymerization reactions can occur under mild conditions without the addition of any catalysts. In addition to the reaction media, the organic solvents play a templating role, making the growth of porous polymer networks proceed under the direction of solvent molecules. As a result, the obtained materials exhibit well-defined micropores with dimensions of solvent molecules. Through the nucleophilic substitution of chloromethylbenzene with ethylene diamine, the frameworks with abundant secondary amines are generated, which offers appropriate adsorbate-adsorbent interaction that is beneficial for selective adsorption and energy-efficient regeneration. The pore structure, together with plentiful amines in frameworks, makes our materials highly active for selective adsorption of CO<sub>2</sub>, whereas CH<sub>4</sub> and N<sub>2</sub> are barely adsorbed. Furthermore, these materials can be completely regenerated under mild conditions, and no loss of activity is observed after six cycles. The low-cost synthesis, high physicochemical stability, outstanding CO<sub>2</sub> selectivity, and energy-saving regeneration make the present porous polymer networks highly promising in selective capture of CO<sub>2</sub> from mixtures such as flue gas and natural gas.

## CONCLUSIONS

A collection of porous polymer networks are fabricated via a nucleophilic substitution reaction of chloromethylbenzene and ethylene diamine. In addition to the reaction media, the solvents also play a templating role that can direct the growth of porous polymer networks. The properties of resultant materials (including polymerization degree, pore structure, and thermal stability) are thus strongly dependent on solvent used. The molecular sizes and polarity can quantitatively reflect the nature of solvents, and correlate well with the properties of materials. Due to the presence of plentiful secondary amines in frameworks and appropriate pore sizes, these materials exhibit high activity in selective capture of CO<sub>2</sub> from gas mixtures containing CH<sub>4</sub> and N<sub>2</sub>. By judicious choice of monomers and solvents, the present strategy should enable secondary amines to be introduced to frameworks with a variety of pore structures and pore sizes, resulting in the fabrication of new porous polymer networks that have great potential for applications in adsorption and catalysis.



## ■ ASSOCIATED CONTENT

### Supporting Information

Fitting parameters, gas chromatographs, adsorption isotherms, micrograph of contact angle, IR spectra of P1, IAST selectivity, nonlinear curve fitting, breakthrough curves, and UV absorption spectra. This material is available free of charge via the Internet at <http://pubs.acs.org>.

## ■ AUTHOR INFORMATION

### Corresponding Authors

\*X.-Q. Liu. E-mail: [liuxq@njtech.edu.cn](mailto:liuxq@njtech.edu.cn).

\*L.-B. Sun. E-mail: [lbsun@njtech.edu.cn](mailto:lbsun@njtech.edu.cn).

### Notes

The authors declare no competing financial interest.

## ■ ACKNOWLEDGMENTS

We acknowledge financial support of this work by the National Basic Research Program of China (973 Program, 2013CB733504), the National High Technology Research and Development Program of China (863 Program, 2013AA032003), Distinguished Youth Foundation of Jiangsu Province (BK20130045), the Fok Ying-Tong Education Foundation (141069), and the Project of Priority Academic Program Development of Jiangsu Higher Education Institutions.

## ■ REFERENCES

- (1) Haszeldine, R. S. Carbon Capture and Storage: How Green Can Black Be? *Science* **2009**, *325*, 1647–1652.
- (2) MacDowell, N.; Florin, N.; Buchard, A.; Hallett, J.; Galindo, A.; Jackson, G.; Adjiman, C. S.; Williams, C. K.; Shah, N.; Fennell, P. An Overview of CO<sub>2</sub> Capture Technologies. *Energy Environ. Sci.* **2010**, *3*, 1645–1669.
- (3) Sumida, K.; Rogow, D. L.; Mason, J. A.; McDonald, T. M.; Bloch, E. D.; Herm, Z. R.; Bae, T. H.; Long, J. R. Carbon Dioxide Capture in Metal-Organic Frameworks. *Chem. Rev.* **2012**, *112*, 724–781.
- (4) Li, J.-R.; Sculley, J.; Zhou, H.-C. Metal-Organic Frameworks for Separations. *Chem. Rev.* **2012**, *112*, 869–932.
- (5) Morris, R. E.; Wheatley, P. S. Gas Storage in Nanoporous Materials. *Angew. Chem., Int. Ed.* **2008**, *47*, 4966–4981.
- (6) D'Alessandro, D. M.; Smit, B.; Long, J. R. Carbon Dioxide Capture: Prospects for New Materials. *Angew. Chem., Int. Ed.* **2010**, *49*, 6058–6082.
- (7) Li, J.-R.; Yu, J.; Lu, W.; Sun, L.-B.; Sculley, J.; Balbuena, P. B.; Zhou, H.-C. Porous Materials with Pre-Designed Single-Molecule Traps for CO<sub>2</sub> Selective Adsorption. *Nat. Commun.* **2013**, *4*, 1538.
- (8) Lu, W.; Sculley, J. P.; Yuan, D.; Krishna, R.; Wei, Z.; Zhou, H.-C. Polyamine-Tethered Porous Polymer Networks for Carbon Dioxide Capture from Flue Gas. *Angew. Chem., Int. Ed.* **2012**, *51*, 7480–7484.
- (9) Shao, X.; Feng, Z.; Xue, R.; Ma, C.; Wang, W.; Peng, X.; Cao, D. Adsorption of CO<sub>2</sub>, CH<sub>4</sub>, CO<sub>2</sub>/N<sub>2</sub> and CO<sub>2</sub>/CH<sub>4</sub> in Novel Activated Carbon Beads: Preparation, Measurements and Simulation. *AIChE J.* **2011**, *57*, 3042–3051.
- (10) Ben, T.; Li, Y.; Zhu, L.; Zhang, D.; Cao, D.; Xiang, Z.; Yao, X.; Qiu, S. Selective Adsorption of Carbon Dioxide by Carbonized Porous Aromatic Framework (PAF). *Energy Environ. Sci.* **2012**, *5*, 8370–8376.
- (11) Hao, G.-P.; Li, W.-C.; Qian, D.; Wang, G.-H.; Zhang, W.-P.; Zhang, T.; Wang, A.-Q.; Schueth, F.; Bongard, H.-J.; Lu, A.-H. Structurally Designed Synthesis of Mechanically Stable Poly-(benzoxazine-co-resol)-based Porous Carbon Monoliths and Their Application as High-Performance CO<sub>2</sub> Capture Sorbents. *J. Am. Chem. Soc.* **2011**, *133*, 11378–11388.
- (12) Reich, T. E.; Behera, S.; Jackson, K. T.; Jena, P.; El-Kaderi, H. M. Highly Selective CO<sub>2</sub>/CH<sub>4</sub> Gas Uptake by a Halogen-Decorated Borazine-Linked Polymer. *J. Mater. Chem.* **2012**, *22*, 13524–13528.
- (13) Lu, W.; Verdegaa, W. M.; Yu, J.; Balbuena, P. B.; Jeong, H.-K.; Zhou, H.-C. Building Multiple Adsorption Sites in Porous Polymer

Networks for Carbon Capture Applications. *Energy Environ. Sci.* **2013**, *6*, 3559–3564.

(14) Filburn, T.; Helble, J. J.; Weiss, R. A. Development of Supported Ethanolamines and Modified Ethanolamines for CO<sub>2</sub> Capture. *Ind. Eng. Chem. Res.* **2005**, *44*, 1542–1546.

(15) Nugent, P.; Belmabkhout, Y.; Burd, S. D.; Cairns, A. J.; Luebke, R.; Forrest, K.; Pham, T.; Ma, S.; Space, B.; Wojtas, L.; Eddaoudi, M.; Zaworotko, M. J. Porous Materials with Optimal Adsorption Thermodynamics and Kinetics for CO<sub>2</sub> Separation. *Nature* **2013**, *495*, 80–84.

(16) Hou, C.; Liu, Q.; Wang, P.; Sun, W.-Y. Porous Metal-Organic Frameworks with High Stability and Selective Sorption for CO<sub>2</sub> over N<sub>2</sub>. *Microporous Mesoporous Mater.* **2013**, *172*, 61–66.

(17) McDonald, T. M.; Lee, W. R.; Mason, J. A.; Wiers, B. M.; Hong, C. S.; Long, J. R. Capture of Carbon Dioxide from Air and Flue Gas in the Alkylamine-Appended Metal-Organic Framework mmen-Mg<sub>2</sub>(dobpdc). *J. Am. Chem. Soc.* **2012**, *134*, 7056–7065.

(18) Burd, S. D.; Ma, S. Q.; Perman, J. A.; Sikora, B. J.; Snurr, R. Q.; Thallapally, P. K.; Tian, J.; Wojtas, L.; Zaworotko, M. J. Highly Selective Carbon Dioxide Uptake by Cu(bpy-n)<sub>2</sub>(SiF<sub>6</sub>) (bpy-1 = 4,4'-Bipyridine; bpy-2 = 1,2-Bis(4-pyridyl)ethene). *J. Am. Chem. Soc.* **2012**, *134*, 3663–3666.

(19) Si, X.; Jiao, C.; Li, F.; Zhang, J.; Wang, S.; Liu, S.; Li, Z.; Sun, L.; Xu, F.; Gabelica, Z.; Schick, C. High and Selective CO<sub>2</sub> Uptake, H<sub>2</sub> Storage and Methanol Sensing on the Amine-Decorated 12-Connected MOF CAU-1. *Energy Environ. Sci.* **2011**, *4*, 4522–4527.

(20) Mason, J. A.; Sumida, K.; Herm, Z. R.; Krishna, R.; Long, J. R. Evaluating Metal-Organic Frameworks for Post-Combustion Carbon Dioxide Capture via Temperature Swing Adsorption. *Energy Environ. Sci.* **2011**, *4*, 3030–3040.

(21) Keskin, S.; van Heest, T. M.; Sholl, D. S. Can Metal-Organic Framework Materials Play a Useful Role in Large-Scale Carbon Dioxide Separations? *ChemSusChem* **2010**, *3*, 879–891.

(22) Krungleviciute, V.; Lask, K.; Migone, A. D.; Lee, J. Y.; Li, J. Kinetics and Equilibrium of Gas Adsorption on RPM1-Co and Cu-BTC Metal-Organic Frameworks: Potential for Gas Separation Applications. *AIChE J.* **2008**, *54*, 918–923.

(23) Yang, Q.; Xue, C.; Zhong, C.; Chen, J.-F. Molecular Simulation of Separation of CO<sub>2</sub> from Flue Gases in Cu-BTC Metal-Organic Framework. *AIChE J.* **2007**, *53*, 2832–2840.

(24) Couck, S.; Denayer, J. F. M.; Baron, G. V.; Remy, T.; Gascon, J.; Kapteijn, F. An Amine-Functionalized MIL-53 Metal Organic Framework with Large Separation Power for CO<sub>2</sub> and CH<sub>4</sub>. *J. Am. Chem. Soc.* **2009**, *131*, 6326–6327.

(25) Long, J. R.; Yaghi, O. M. The Pervasive Chemistry of Metal-Organic Frameworks. *Chem. Soc. Rev.* **2009**, *38*, 1213–1214.

(26) Furukawa, H.; Yaghi, O. M. Storage of Hydrogen, Methane, and Carbon Dioxide in Highly Porous Covalent Organic Frameworks for Clean Energy Applications. *J. Am. Chem. Soc.* **2009**, *131*, 8875–8883.

(27) Martin, C. F.; Stockel, E.; Clowes, R.; Adams, D. J.; Cooper, A. I.; Pis, J. J.; Rubiera, F.; Pevida, C. Hypercrosslinked Organic Polymer Networks as Potential Adsorbents for Pre-Combustion CO<sub>2</sub> Capture. *J. Mater. Chem.* **2011**, *21*, 5475–5483.

(28) Jiang, J.-X.; Su, F.; Trewin, A.; Wood, C. D.; Campbell, N. L.; Niu, H.; Dickinson, C.; Ganin, A. Y.; Rosseinsky, M. J.; Khimyak, Y. Z.; Cooper, A. I. Conjugated Microporous Poly (aryleneethynylene) Networks. *Angew. Chem., Int. Ed.* **2007**, *46*, 8574–8578.

(29) Weber, J.; Su, O.; Antonietti, M.; Thomas, A. Exploring Polymers of Intrinsic Microporosity-Microporous, Soluble Polyamide and Polyimide. *Macromol. Rapid Commun.* **2007**, *28*, 1871–1876.

(30) Liebl, M. R.; Senker, J. Microporous Functionalized Triazine-based Polyimides with High CO<sub>2</sub> Capture Capacity. *Chem. Mater.* **2013**, *25*, 970–980.

(31) Ben, T.; Pei, C.; Zhang, D.; Xu, J.; Deng, F.; Jing, X.; Qiu, S. Gas Storage in Porous Aromatic Frameworks (PAFs). *Energy Environ. Sci.* **2011**, *4*, 3991–3999.

(32) Rabbani, M. G.; El-Kaderi, H. M. Template-Free Synthesis of a Highly Porous Benzimidazole-Linked Polymer for CO<sub>2</sub> Capture and H<sub>2</sub> Storage. *Chem. Mater.* **2011**, *23*, 1650–1653.

- (33) Peng, X.; Cao, D. Computational Screening of Porous Carbons, Zeolites, and Metal Organic Frameworks for Desulfurization and Decarburization of Biogas, Natural Gas, and Flue Gas. *AIChE J.* **2013**, *59*, 2928–2942.
- (34) Xu, C.; Hedin, N. Synthesis of Microporous Organic Polymers with High CO<sub>2</sub>-over-N<sub>2</sub> Selectivity and CO<sub>2</sub> Adsorption. *J. Mater. Chem. A* **2013**, *1*, 3406–3414.
- (35) Zhao, H.; Jin, Z.; Su, H.; Zhang, J.; Yao, X.; Zhao, H.; Zhu, G. Target Synthesis of a Novel Porous Aromatic Framework and Its Highly Selective Separation of CO<sub>2</sub>/CH<sub>4</sub>. *Chem. Commun.* **2013**, *49*, 2780–2782.
- (36) Thomas, A. Functional Materials: From Hard to Soft Porous Frameworks. *Angew. Chem., Int. Ed.* **2010**, *49*, 8328–8344.
- (37) Qian, H.; Zheng, J.; Zhang, S. Preparation of Microporous Polyamide Networks for Carbon Dioxide Capture and Nanofiltration. *Polymer* **2013**, *54*, 557–564.
- (38) Ben, T.; Ren, H.; Ma, S.; Cao, D.; Lan, J.; Jing, X.; Wang, W.; Xu, J.; Deng, F.; Simmons, J. M.; Qiu, S.; Zhu, G. Targeted Synthesis of a Porous Aromatic Framework with High Stability and Exceptionally High Surface Area. *Angew. Chem., Int. Ed.* **2009**, *48*, 9457–9460.
- (39) Stavitski, E.; Pidko, E. A.; Couck, S.; Remy, T.; Hensen, E. J. M.; Weckhuysen, B. M.; Denayer, J.; Gascon, J.; Kapteijn, F. Complexity Behind CO<sub>2</sub> Capture on NH<sub>2</sub>-MIL-53(Al). *Langmuir* **2011**, *27*, 3970–3976.
- (40) Lu, W.; Yuan, D.; Sculley, J.; Zhao, D.; Krishna, R.; Zhou, H.-C. Sulfonate-Grafted Porous Polymer Networks for Preferential CO<sub>2</sub> Adsorption at Low Pressure. *J. Am. Chem. Soc.* **2011**, *133*, 18126–18129.
- (41) Hao, G.-P.; Li, W.-C.; Qian, D.; Lu, A.-H. Rapid Synthesis of Nitrogen-Doped Porous Carbon Monolith for CO<sub>2</sub> Capture. *Adv. Mater.* **2010**, *22*, 853–857.
- (42) Monazam, E. R.; Shadle, L. J.; Miller, D. C.; Pennline, H. W.; Fauth, D. J.; Hoffman, J. S.; Gray, M. L. Equilibrium and Kinetics Analysis of Carbon Dioxide Capture Using Immobilized Amine on a Mesoporous Silica. *AIChE J.* **2013**, *59*, 923–935.
- (43) Lu, W.; Sculley, J. P.; Yuan, D.; Krishna, R.; Zhou, H.-C. Carbon Dioxide Capture from Air Using Amine-Grafted Porous Polymer Networks. *J. Phys. Chem. C* **2013**, *117*, 4057–4061.
- (44) Zhu, Y.; Long, H.; Zhang, W. Imine-Linked Porous Polymer Frameworks with High Small Gas (H<sub>2</sub>, CO<sub>2</sub>, CH<sub>4</sub>, C<sub>2</sub>H<sub>2</sub>) Uptake and CO<sub>2</sub>/N<sub>2</sub> Selectivity. *Chem. Mater.* **2013**, *25*, 1630–1635.
- (45) Wang, H.-B.; Jessop, P. G.; Liu, G. Support-Free Porous Polyamine Particles for CO<sub>2</sub> Capture. *ACS Macro Lett.* **2012**, *1*, 944–948.
- (46) Schwab, M. G.; Fassbender, B.; Spiess, H. W.; Thomas, A.; Feng, X.; Muellen, K. Catalyst-Free Preparation of Melamine-based Microporous Polymer Networks through Schiff Base Chemistry. *J. Am. Chem. Soc.* **2009**, *131*, 7216–7217.
- (47) Monazam, E. R.; Shadle, L. J.; Siriwardane, R. Equilibrium and Absorption Kinetics of Carbon Dioxide by Solid Supported Amine Sorbent. *AIChE J.* **2011**, *57*, 3153–3159.
- (48) Liu, Y.; Ye, Q.; Shen, M.; Shi, J.; Chen, J.; Pan, H.; Shi, Y. Carbon Dioxide Capture by Functionalized Solid Amine Sorbents with Simulated Flue Gas Conditions. *Environ. Sci. Technol.* **2011**, *45*, 5710–5716.
- (49) Liu, L.; Li, P.-z.; Zhu, L.; Zou, R.; Zhao, Y. Microporous Polymelamine Network for Highly Selective CO<sub>2</sub> Adsorption. *Polymer* **2013**, *54*, 596–600.
- (50) Neti, V. S. P. K.; Wu, X.; Deng, S.; Echegoyen, L. Selective CO<sub>2</sub> Capture in an Imine Linked Porphyrin Porous Polymer. *Polym. Chem.* **2013**, *4*, 4566–4569.
- (51) Choi, H. J.; Park, Y. S.; Yun, S. H.; Kim, H. S.; Cho, C. S.; Ko, K.; Ahn, K. H. Novel C<sub>3v</sub>-Symmetric Tripodal Scaffold, Triethyl cis,cis,cis-2,5,8-Tribenzyltrindane-2,5,8-Tricarboxylate, for the Construction of Artificial Receptors. *Org. Lett.* **2002**, *4*, 795–798.
- (52) Rowsell, J. L. C.; Yaghi, O. M. Effects of Functionalization, Catenation, and Variation of the Metal Oxide and Organic Linking Units on the Low-Pressure Hydrogen Adsorption Properties of Metal-Organic Frameworks. *J. Am. Chem. Soc.* **2006**, *128*, 1304–1315.
- (53) Jiang, W.-J.; Yin, Y.; Liu, X.-Q.; Yin, X.-Q.; Shi, Y.-Q.; Sun, L.-B. Fabrication of Supported Cuprous Sites at Low Temperatures: An Efficient, Controllable Strategy Using Vapor-Induced Reduction. *J. Am. Chem. Soc.* **2013**, *135*, 8137–8140.
- (54) Myers, A.; Prausnitz, J. Thermodynamics of Mixed-Gas Adsorption. *AIChE J.* **1965**, *11*, 121–127.
- (55) Reichardt, C. Solvatochromic Dyes as Solvent Polarity Indicators. *Chem. Rev.* **1994**, *94*, 2319–2358.
- (56) Totten, R. K.; Kim, Y.-S.; Weston, M. H.; Farha, O. K.; Hupp, J. T.; Nguyen, S. T. Enhanced Catalytic Activity through the Tuning of Micropore Environment and Supercritical CO<sub>2</sub> Processing: Al-(Porphyrin)-based Porous Organic Polymers for the Degradation of a Nerve Agent Simulant. *J. Am. Chem. Soc.* **2013**, *135*, 11720–11723.
- (57) Weber, J.; Schmidt, J.; Thomas, A.; Boehlmann, W. Micropore Analysis of Polymer Networks by Gas Sorption and Xe-129 NMR Spectroscopy: Toward a Better Understanding of Intrinsic Microporosity. *Langmuir* **2010**, *26*, 15650–15656.
- (58) Xu, Q.; Yang, Y.; Wang, X.; Wang, Z.; Jin, W.; Huang, J.; Wang, Y. Atomic Layer Deposition of Alumina on Porous Polytetrafluoroethylene Membranes for Enhanced Hydrophilicity and Separation Performances. *J. Membr. Sci.* **2012**, *415–416*, 435–443.
- (59) Huang, F. L.; Wang, Q. Q.; Wei, Q. F.; Gao, W. D.; Shou, H. Y.; Jiang, S. D. Dynamic Wettability and Contact Angles of Poly(vinylidene fluoride) Nanofiber Membranes Grafted with Acrylic Acid. *Express Polymer Lett.* **2010**, *4*, 551–558.
- (60) Dawson, R.; Adams, D. J.; Cooper, A. I. Chemical Tuning of CO<sub>2</sub> Sorption in Robust Nanoporous Organic Polymers. *Chem. Sci.* **2011**, *2*, 1173–1177.
- (61) Mohanty, P.; Kull, L. D.; Landskron, K. Porous Covalent Electron-Rich Organonitridic Frameworks as Highly Selective Sorbents for Methane and Carbon Dioxide. *Nat. Commun.* **2011**, *2*, 401.
- (62) Lu, W.; Yuan, D.; Zhao, D.; Schilling, C. I.; Plietzsch, O.; Muller, T.; Braese, S.; Guenther, J.; Bluemel, J.; Krishna, R.; Li, Z.; Zhou, H.-C. Porous Polymer Networks: Synthesis, Porosity, and Applications in Gas Storage/Separation. *Chem. Mater.* **2010**, *22*, 5964–5972.
- (63) Herm, Z. R.; Swisher, J. A.; Smit, B.; Krishna, R.; Long, J. R. Metal-Organic Frameworks as Adsorbents for Hydrogen Purification and Precombustion Carbon Dioxide Capture. *J. Am. Chem. Soc.* **2011**, *133*, 5664–5667.
- (64) Cavenati, S.; Grande, C. A.; Rodrigues, A. E. Adsorption Equilibrium of Methane, Carbon Dioxide, and Nitrogen on Zeolite 13X at High Pressures. *J. Chem. Eng. Data* **2004**, *49*, 1095–1101.
- (65) Saleh, M.; Tiwari, J. N.; Kemp, K. C.; Yousuf, M.; Kim, K. S. Highly Selective and Stable Carbon Dioxide Uptake in Polyindole-Derived Microporous Carbon Materials. *Environ. Sci. Technol.* **2013**, *47*, 5467–5473.
- (66) Huang, Y.; Xu, Y.; He, Q.; Du, B.; Cao, Y. Preparation and Characteristics of a Dummy Molecularly Imprinted Polymer for Phenol. *J. Appl. Polym. Sci.* **2013**, *128*, 3256–3262.
- (67) Zhu, Q.; Huang, D.; Li, L.; Yin, Y. Synthesis of Molecularly Imprinted Polymers for the Application of Selective Clean-up Vinblastine from Catharanthus Roseus Extract. *Sci. Chin. Chem.* **2010**, *53*, 2587–2592.